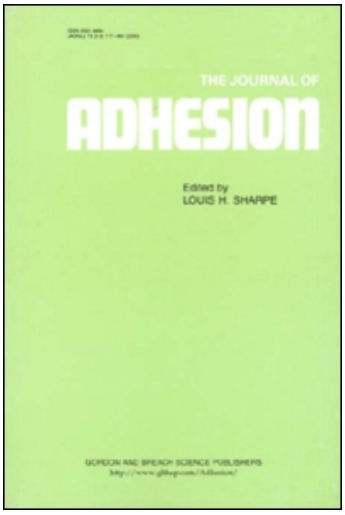

The Journal of Adhesion
Publication details, including instructions for authors and subscription information:
http://www.informaworld.com/smpp/title~content=t713453635

An Elasto-Plastic Investigation of the Peel Test

A. D. Crocombe[a]; R. D. Adams[a]
[a] Department of Mechanical Engineering, University of Bristol, Bristol, England

To cite this Article Crocombe, A. D. and Adams, R. D.(1982) 'An Elasto-Plastic Investigation of the Peel Test', The Journal of Adhesion, 13: 3, 241 — 267
To link to this Article: DOI: 10.1080/00218468208073190
URL: http://dx.doi.org/10.1080/00218468208073190

J. Adhesion, 1982, Vol. 13, pp. 241–267
0021–8464/82/1304–0241 $06.50/0

Printed in Great Britain

An Elasto-Plastic Investigation of the Peel Test

A. D. CROCOMBE and R. D. ADAMS†

Department of Mechanical Engineering, University of Bristol, Bristol BS8 1TR, England

(Received September 12, in final form October 6 1981)

This work outlines an elasto-plastic investigation of two common peel tests which use high and low yield strength aluminium adherends. An elastic, large-displacement, finite element program has been extended to include elasto-plastic material behaviour. This has been used to analyse both peel tests. The adhesive stresses near the crack tip have been shown to be finite while the corresponding strains remain singular. A failure criterion based on a maximum adhesive strain has been used to predict the relative strengths of the peel test. The amount of energy dissipated in the plastic deformation of the peeling adherends has been assessed by a series of tests and has been shown to be a considerable amount of the total energy supplied to the peeling system. Further, although the two aluminium alloys considered have grossly different yield strengths the energies dissipated in plastic deformation are similar. Material data for the finite element analysis and the plastic work calculations have been obtained from uniaxial tensile tests of both the adherends and the adhesive and actual peel strengths have been measured in a series of peel tests.

NOTATION

General symbols

$[\ ]$	Square brackets around a quantity denote an array
$\underline{\ }$	Bar over a quantity denotes a column vector

Variables

$\bar{a}$	Yield function derivatives
A_κ	Variable used in derivation of the elasto-plastic modulus
$[B]$	Incremental strain-displacement array
$\bar{D}$	Displacement vector
$[D_{ep}]$	Elasto-plastic modulus array
$f(\sigma)$	Yield function
$F(\sigma)$	Yield surface

† To whom any communication should be addressed.

$[G]$	Shape function derivative array
J_1, J_2	Stress invariants
$[K_T]$	Tangential stiffness array
m	Moment arm
M	Bending moment
M_p	Bending moment to cause total yield
P	Applied load/unit width
P_P, P_F	Loads defined in plastic work measurements
R	Radius of curvature
$\bar{R}$	Load vector
S	Ratio of yield in tension and compression
$[S]$	Stress array
T	Thickness
u, v, w	Displacement along cartesian co-ordinates
V	Volume
x, y, z	Cartesian co-ordinates
Y	Yield stress
$\bar{\delta}$	Displacement vector
ε	Direct strain
$\bar{\varepsilon}$	Strain vector
κ	Hardening parameter
$d\lambda$	Plastic multiplier
σ	Direct stress
$\bar{\sigma}$	Stress vector
ϕ	Actual peel angle
$\bar{\psi}$	Residual vector
Ψ	Plastic energy
$\bar{\emptyset}$	Zero vector

Subscripts (unless otherwise specified)

a	Adherend
C	Compression
eff	Effective plastic
p	Plastic
prin	Principal
T	Tension
x, y, z	Co-ordinate direction

INTRODUCTION

An adhesive bond is inherently weak when it is subjected to cleavage (or peel) loads. For this reason, the peel test was developed to compare the performance of adhesives under this type of loading. It exists in a number of forms but all are variations of a common theme shown schematically in Figure 1.

This work is an extension of a previous investigation[1] which considered purely elastic behaviour of the adherend and adhesive. These studies have been undertaken to allow a more meaningful interpretation of peel test results and, ultimately, to establish a correlation between the various adhesive tests. Among the conclusions drawn from the large displacement, elastic analysis of

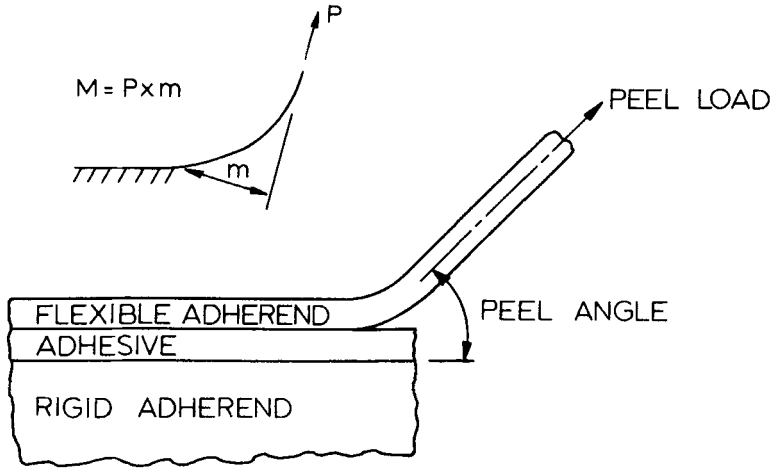

FIGURE 1 Schematic representation of the peel test.

the peel test[1] was that the peel test was non-linear, a small increase in adhesive strength requiring a much larger increase in peel load. The flexible adherend in most peel tests is metallic (usually aluminium) and so a certain amount of plastic behaviour in both adhesive and adherend is likely to occur before failure. It is felt that this plastic behaviour, particularly in the flexible adherend, will further increase the non-linearity of the peel test. As the adhesive strength is increased, proportionately more work is required to deform the aluminium, thus resulting in higher peel loads. Also, because different peel tests use different flexible adherends, comparison of results can be difficult. For example, one British peel test[2] uses a soft aluminium (with a low yield strength) while an American counterpart[3] uses an aluminium with a high yield strength (details of both are given later). The varying amount of plastic deformation may affect the recorded peel strengths considerably and hence the assessment of the adhesive performance.

Although a number of workers[4–9] have attempted qualitatively to include the effects of plasticity, the assumptions involved in the various ideal plasticity models limit their general application and imply that "no complete peel analysis can exist..."[7]. Spies[5] was the first to include plastic effects, by defining effective adhesive and adherend moduli to account for the elasto-plastic behaviour observed. Bikerman[4] allowed the adhesive to follow a non-linear stress-strain curve and so effectively treated the adhesive as a series of springs with non-linear rates. Duke and Stanbridge[6] found that plastic deformation of the adherend in their peel test was a prerequisite for steady peeling, rather than catastrophic failure. Further, by comparing the expression for the maximum

adherend bending moment from an elastic analysis with that required to cause flexural yield in the strip, they showed that, for a particular system, there is a critical adherend thickness above which no plastic behaviour (and hence no steady peeling) will occur. In a subsequent piece of work Duke[7] modelled the adhesive as having reached its maximum (yield) value over a small distance at the end of the joint and was able to predict the bend radius of the adherend at various adherend thicknesses. Finally, Wang and Vazirani[9] modelled plastic yielding of polythene bonded with an epoxy to a copper base as a reverse of the indentation problem of Prandtl and used this to explain the series of ridges of yielded polythene.

From the above it is clear that although the importance of plastic behaviour is recognised, no general treatment of the problem exists. Analysis of the peel test is carried out here by extending a large displacement, elastic finite element program to include elasto-plastic material behaviour.

THEORETICAL BACKGROUND

A brief outline of the development of the non-linear, finite element program is given below; further details can be found in Ref. 10.

Large Displacement Theory

Large *displacement* theory is a simplification of the general large *deformation* theory when the material strains are small. Such behaviour is found in the deflection of slender beams such as the flexible adherend of the peel test. The general strain-displacement equation is given as:

$$2\varepsilon_{p,q} = \frac{\partial D_p}{\partial q} + \frac{\partial D_q}{\partial p} + \left[\frac{\partial \bar{D}}{\partial p} \cdot \frac{\partial \bar{D}}{\partial q}\right]$$

where $p, q = x, y, z$

$$\bar{D} = u\bar{i} + v\bar{j} + w\bar{k}.$$

For the direct strains in the x-direction (ε_x) this can be written:

$$\varepsilon_x = \frac{\partial u}{\partial x} + \frac{1}{2}\left(\left(\frac{\partial u}{\partial x}\right)^2 + \left(\frac{\partial v}{\partial x}\right)^2 + \left(\frac{\partial w}{\partial x}\right)^2\right)$$

and it can be seen that this is an extension of the small displacement, strain-displacement equation ($\varepsilon_x = du/dx$) including the squares of the displacement derivatives and it is these terms that introduce the geometric non-linearities.

PLASTICITY THEORY

Yield surfaces

Plastic deformation during loading occurs when there is a permanent change of shape. Material is assumed to yield plastically when some function of the stress state ($f(\sigma)$), known as the yield function, reaches a critical level (Y). This can be represented generally as

$$F(\sigma) = f(\sigma) - Y = 0$$

$F(\sigma)$ is known as the yield surface, all stress states within this surface being elastic. The yield function can be represented as a function of the stress invariants J_1 and J_2 where

$$J_1 = \sigma_x + \sigma_y + \sigma_z$$

$$J_2 = \tfrac{1}{2}(\sigma_x'^2 + \sigma_y'^2 + \sigma_z'^2) + \tau_{xy}^2 + \tau_{xz}^2 + \tau_{yz}^2$$

and

$$\sigma_x' = \sigma_x - J_1/3$$

J_1 is a measure of the hydrostatic level of stress and J_2 the deviatoric level.

In general, different materials require different yield functions. In this work, the von Mises yield function has been used to model the yielding of the aluminium and a modified (paraboloidal) von Mises yield function used for the adhesive. These are expressed in terms of J_1 and J_2 (after Raghava[11] and Peppiatt[12])

$$F(\sigma) = (3J_2)^{1/2} - Y_T$$

$$F(\sigma) = (J_1(S-1) + (J_1^2(S-1)^2 + 12J_2S)^{1/2})/2S - Y_T$$

where

Y_T = the yield stress in tension
S = the ratio of yield stress in tension and compression.

It can be seen that the former is a function of the deviatoric stresses only while the latter depends on both the deviatoric and hydrostatic stresses. When S is unity the two criteria are the same.

Work hardening

Materials seldom yield at a constant stress (ideally plastic); often they support increased load as they yield. This aspect is known as work hardening and can be modelled by changing the yield surface. For the von Mises and modified von Mises yield surfaces this can be achieved by increasing the yield stress (Y_T).

This causes the yield surface to expand uniformly and is known as isotropic hardening. The value of Y_T is obtained from the uniaxial stress-strain curve at an appropriate equivalent strain. Assuming a work hardening process, this equivalent strain is the strain that causes the same amount of plastic work as that experienced by the system being analysed. Thus, a general form for the yield surface is:

$$F = f(\sigma) - Y_T(\kappa)$$

where κ is some hardening parameter.

Plastic stress-strain relations

Straining during yielding can be split into elastic and plastic components.

$$\bar{\varepsilon} = \bar{\varepsilon}_e + \bar{\varepsilon}_p$$

The elastic components of the strain can be obtained directly from the stresses using the Hookean relationship of elasticity. Plastic increments of the strain can be obtained using a flow rule[13] which states that the increment of plastic strain is proportional to the yield function derivative. This can be written as:

$$d\bar{\varepsilon}_p = d\lambda(\overline{\partial f/\partial \sigma})$$

Geometric and Material Non-Linearities and the Finite Element Method

Details of the basic finite element principles can be found in Ref. 14 and further information on the non-linear aspects can be found in Ref. 10.

The finite element method seeks to solve the equation

$$\bar{\psi} = \bar{R} - \int [B]^T \bar{\sigma}\, dV = \bar{\emptyset}$$

where $\bar{\psi}$ is the residual vector
$\bar{R}$ is the load vector
$[B]$ is the incremental strain-displacement array
$\bar{\sigma}$ is the stress vector
$\bar{\emptyset}$ is a zero vector

The incremental stress vector is given by

$$d\bar{\sigma} = [D_{\text{ep}}][B]\, d\bar{\delta}$$

where $[D_{\text{ep}}]$ is the modulus array
$\bar{\delta}$ is the displacement vector

When modelling large displacements and elasto-plastic behaviour, the incremental strain-displacement array ($[B]$) and modulus array ($[D_{\text{ep}}]$)

respectively are functions of the displacements. Thus it is necessary to solve a non-linear equation

$$\bar{\psi}(\delta) = \bar{\emptyset}$$

This is achieved using a type of Newton–Raphson approach obtaining successively better approximations to the displacements ($\bar{\delta}$) as

$$\bar{\delta}_{i+1} = \bar{\delta}_i - \bar{\psi}_i [K_T]_i^{-1}$$

where $[K_T]$ is $\int([B]^T[D_{ep}][B]+[G]^T[S][G])dv$
$[S]$ is an array of the stresses
$[G]$ is an array of the shape function derivatives.

The only difference between this approach and that used in the previous large displacement, elastic analysis is the introduction of $[D_{ep}]$ an array linking an elasto-plastic increment of stress to the strain. It can be shown[10,15] that

$$[D_{ep}] = [[D] - ([D]\bar{s} \rightarrow \bar{a}^T[D])/(A_\kappa + \bar{a}^T[D]\bar{a})]$$

where $[D]$ is the elastic modulus array
$\bar{a}$ is the vector of yield function derivatives
A_κ is the appropriate slope of the stress-plastic strain curve of the material concerned.

By using the above approach, a solution to the general, large-displacement, elasto-plastic, finite element analysis can be obtained and appropriate details are given in Ref. 10.

OUTLINE OF THE INVESTIGATION

This investigation has been based on the American[3] and British[2] peel tests mentioned earlier, referred to as peel tests A and B respectively. Peel test A uses a relatively strong aluminium alloy (2024-T3) while peel test B uses a much softer, manganese-aluminium alloy (B.S.3L61). The adhesive used is a rubber modified epoxy based on a diglyicidyl ether of bisphenol-A together with 15 parts per hundred of resin (pphr) of carboxyl-terminated butadiene-acrylonitrile rubber and 5 pphr of piperidine as the curing agent. This system has been used by other workers[16] and is known to have a high resistance to fracture.

Work in this investigation falls into three sections. The first involves carrying out a series of controlled peel tests, using both types of aluminium to establish the appropriate peel strengths. In the next section, the amount of work involved in plastically deforming the aluminium in the 90° peel test is assessed in an attempt to establish how much of the total energy supplied to

the peeling system is actually used in the adhesive fracturing process. The final section involves a full non-linear elasto-plastic finite element analysis of the peeling configurations tested in the first section. Both of these last two sections require information on the elasto-plastic behaviour of the materials involved. The required form for this information is uniaxial stress-strain curves and details of the testing of the two types of aluminium and the adhesive is given below.

MATERIAL UNIAXIAL TENSILE TESTS

Aluminium Tests

Specimens of both types of aluminium, B.S.3L61 and 2024-T3, were machined to the British Standard specification (B.S.18). These were then tested under quasi-static conditions in a Hounsfield tensometer. True stress-strain curves for the two aluminiums were obtained, Figures 2 and 3, assuming a Poisson's ratio of 0.5. Using this value considerably simplified true stress computations while only introducing errors of less than 0.3%. By fitting a least squares, cubic spline[17] curve to the data points (solid line on Figures 2 and 3), and assuming

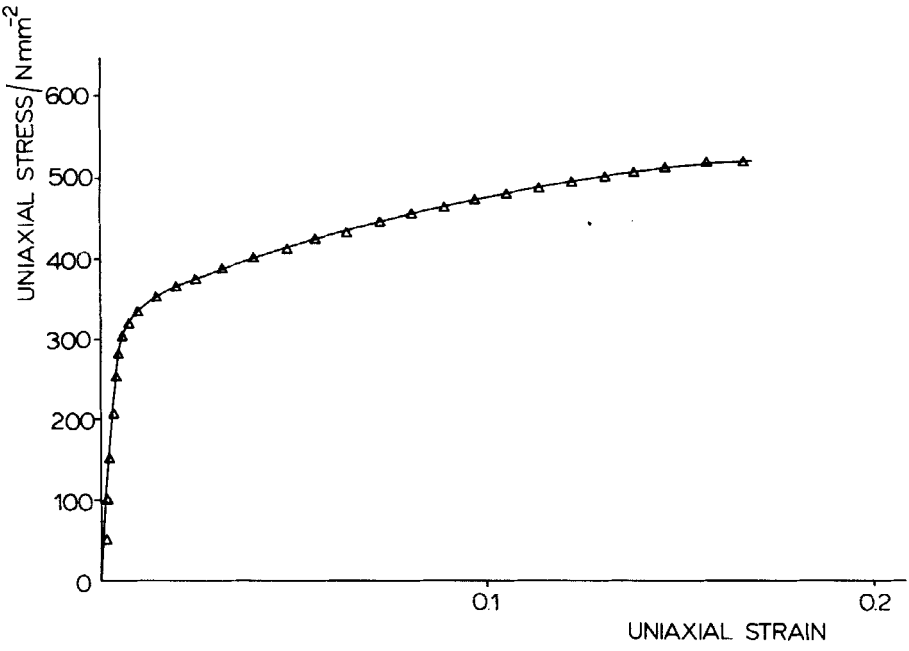

FIGURE 2 True stress-strain curve for aluminium 2024-T3.

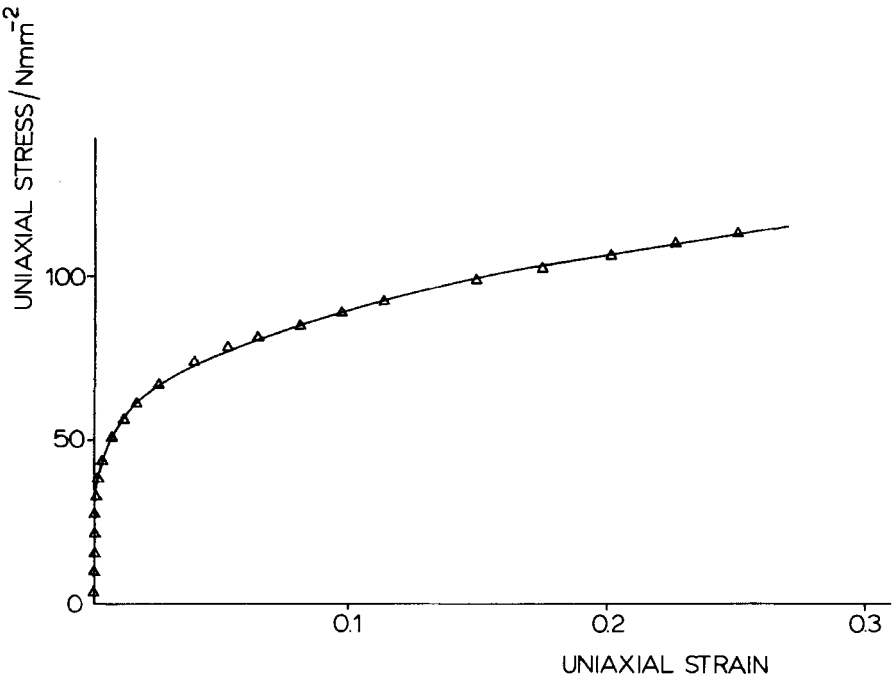

FIGURE 3 True stress-strain curve for aluminium BS 3L61.

yield to occur at a proof stress corresponding to the strain at the end of the linear region of the stress-strain curve, yield stresses of 34.4 and 308.7 N mm^{-2} were obtained for the two aluminiums. This latter value is in agreement with the specified value of 311 N mm^{-2} (there is no yield stress given in the specification of the softer aluminium). The cubic spline curve fitting technique[17] is a method of defining a curve over a whole region by separate cubic polynomials over parts of the region. Each polynomial has the same value and first and second derivatives at their common boundaries.

Adhesive Tests

Blocks of the cured rubber modified epoxy were machined to B.S.18 proportions. Having been polished with a proprietary metal polish, they were tested at different rates in a 30 kN capacity, screw driven, testing machine. Extension of the gauge length was measured using a modification of the Martens extensometer in which two displacement transducers (LVDT's) are mounted in lever systems on opposite sides of the specimen. The surface of the

adhesive specimen was protected by a layer of varnish. While testing the specimens, bending was assessed by monitoring the strains on opposite sides of the specimen. These were within $\pm 2\%$ and indicated minimal bending.

Two different rates of testing were used and these resulted in times to failure of about 200 sec and 14 sec. True stress-strain curves from these tests, Figure 4, were obtained by assuming a value of Poisson's ratio of 0.5, only introducing errors of about 0.6% in the true stress computations. From these curves it can be seen that although the time to failure is decreased by more than an order of magnitude, the value of the maximum stress only increases by about 10%. Based on elastic considerations and allowing for adhesive yielding, the faster

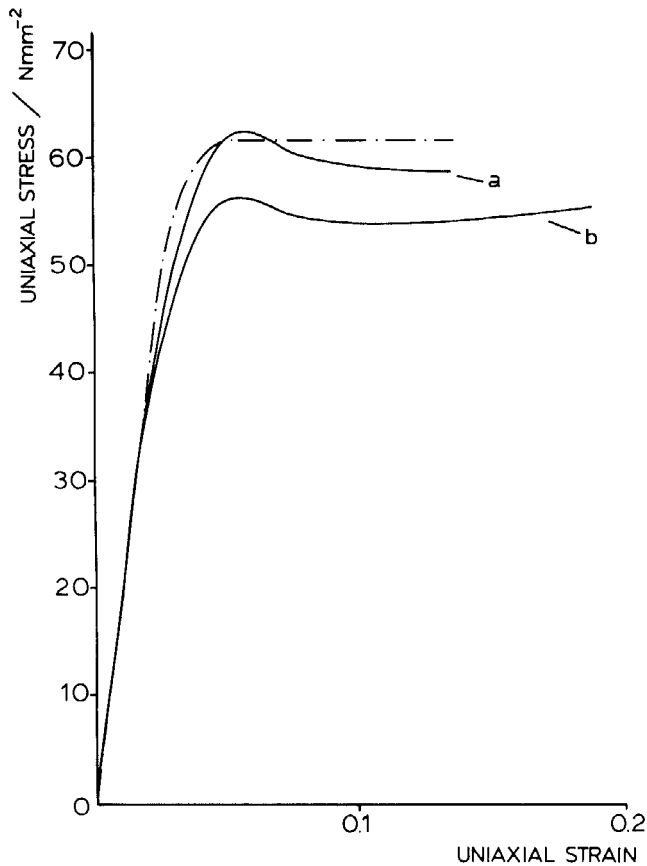

FIGURE 4 True stress-strain curves for rubber modified epoxy tested at different rates (mean times to failure of: (a) 14 sec; (b) 200 sec).

time to failure would seem to be representative of the rate of loading experienced by the adhesive in the series of peel tests outlined later.

The cubic spline model of this material data, used in the subsequent finite element analysis of the peel test, is shown (as a broken line) in Figure 4. The use of a proof stress to define yield in polymers has been outlined by Raghava[11] ("offset stress"), and in this work, by arbitrarily defining a 0.5% proof stress, yield occurs at about 52 N mm^{-2}. It has been found that changing this value of the proof stress does not significantly affect the results from the analysis of the peel test. An average value of the tensile modulus of 2008 N mm^{-2} was obtained from the adhesive tests at the higher rate and this has been used in the subsequent analysis.

PEEL TESTS

Manufacture

Peel test specimens 10 mm wide with flexible and "rigid" adherend lengths of 150 and 90 mm respectively were made by bonding sheets, of the appropriate materials, 150 mm wide, and guillotining to the final width. The base material was stock aluminium alloy sheet, 1.6 mm thick (which, during testing, is bonded to a steel base plate) and the thinner, flexible adherends were aluminium alloy, either to B.S.3L61 specification, 0.57 mm thick, or 2024-T3 and 0.64 mm thick. (These are the materials specified by the American[3] and British[2] peel tests respectively.) All the adherends were subjected to a standard sulphuric acid etch. The cure schedule for the particular adhesive used was 16 h at 120°C followed by a slow cool to room temperature. Ten peel test specimens were obtained from each bonded sheet. A quick-setting adhesive was used to bond each specimen to a steel base plate. This base plate was then clamped into the peel test rig which was attached to the base of a testing machine (Figure 5) using linear bearings. These bearings allowed free movement in the sense indicated in the figure and hence enabled the rig to align itself during testing, thus maintaining a constant peel angle. The peel angle was set by rotating the carried plate and the specimen peeled by the upward movement of the top crosshead.

Test Procedure and Results

Peel tests at angles of 90, 60 and 30 degrees were made. With a constant angle of peel and small adherend straining the separation rate in the peel test is controlled by the crosshead speed only. Crosshead speeds were set to give a separation rate of 10 mm min^{-1} and by peeling a specimen along only part of its length it could be used for a number of tests.

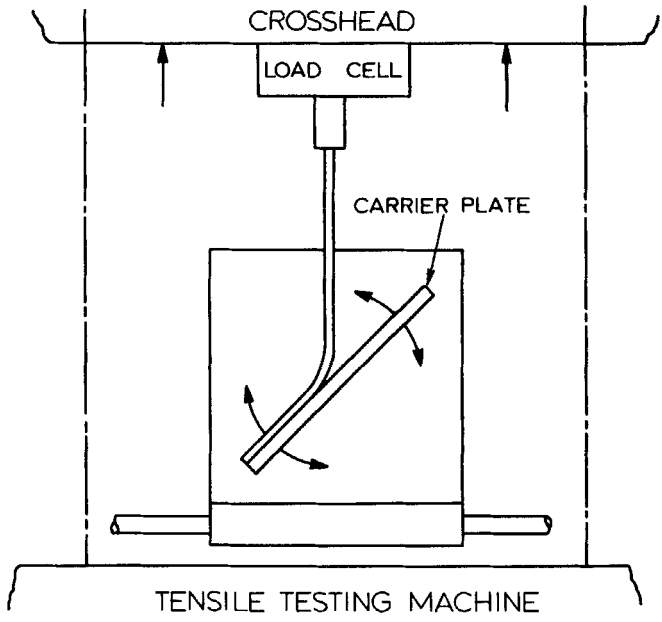

FIGURE 5 Schematic representation of peel test rig.

A summary of the results for both peel tests is shown in Figure 6. All the failures were clearly cohesive in nature, failing near the adhesive-flexible adherend interface but leaving a visible layer of adhesive on the adherend. Clearly, values of peel strength increase with decreasing peel angle, and the differences between the two tests decrease. At 90°, the peel strength from A is 29% lower than that from B while at 30°, the peel strength from A is 4% higher than that from B. Possible reasons for this trend are discussed later when considering elasto-plastic analysis of the peel test.

PLASTIC BENDING TESTS OF THE ALUMINIUM

These were carried out to assess the energy dissipated in the bending and unbending of the aluminium in the A and B 90° peel tests.

Description of Equipment

The apparatus used is shown schematically in Figure 7. The base of a longitudinal air bearing was clamped to the testing machine. An aluminium

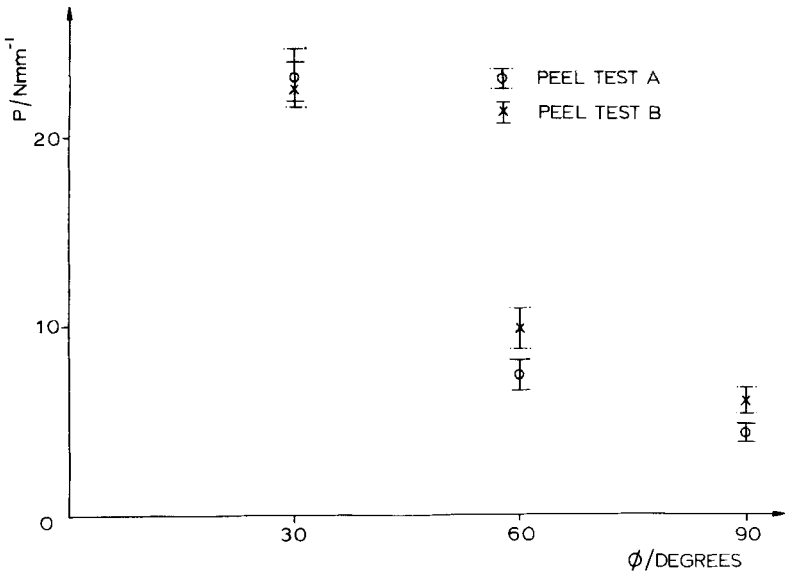

FIGURE 6 Results from peel test, plotting peel load (P) against peel angle (ϕ).

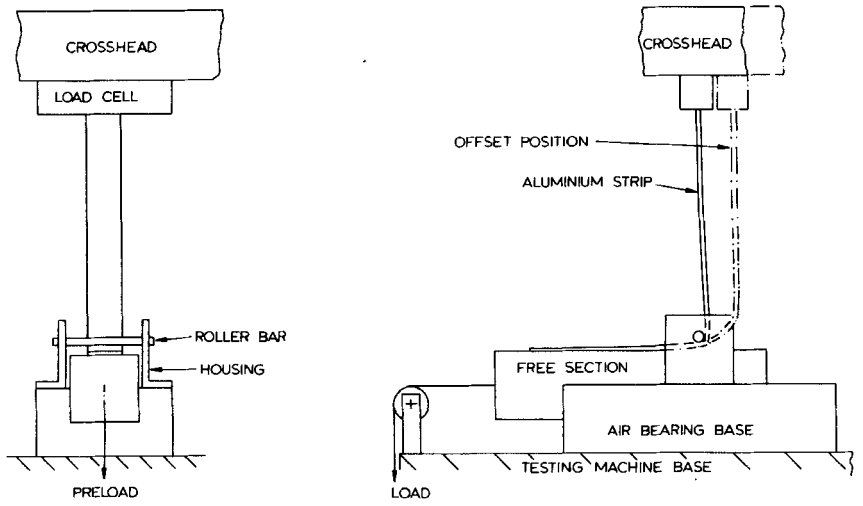

FIGURE 7 Schematic representation of apparatus used to determine energy dissipated in plastic bending.

strip, of the same material and width as the flexible adherend in the peel test, was fixed to the free member of this bearing, passed under the roller bar and attached to the load cell. This load cell was mounted on the crosshead of the testing machine and measured the forces generated as the crosshead moves away from the machine base, bending the aluminium strip around the roller bar. The work expended in plastic deformation of this strip is a product of the load and the distance moved.

Preloading the free member of the bearing causes a higher load in the strip (analogous to increasing the peel load) which causes greater deformation in the adherend. By varying the amount of preload, it is possible to obtain a series of values for the work dissipated in plastic deformation at various peel loads. The value of the plastic work (Ψ) for a unit distance movement of the strip is

$$\Psi = (P - P_P - P_F) \times 1$$

where P = load measured at the load cell
P_P = preload value
P_F = frictional load at the bearings.

By replacing the aluminium strip with a strong cord and repeating the procedure for various preloads (P_P), values of the frictional forces (P_F) have been obtained. These have been used in the above expression to evaluate the plastic work expended in bending the strip. At full load the frictional loads are only about 6% of the measured loads.

Test Procedure and Results

These tests were carried out for the aluminiums used in peel tests A and B, up to a maximum load of 5 N mm^{-1}. This corresponds to the observed 90° peel strengths outlined above. Results for the two materials are shown in Figure 8. It can be seen that the work dissipated in plastic bending increases linearly with applied load at similar rates for both materials. Although the work expended in plastic deformation, at a given load, is higher in the 2024-T3 aluminium, it is a considerable proportion of the total energy supplied in both cases.

These results were obtained with the roller bar and load cell vertically in line (see Figure 7). Clearly, this overconstrains the stronger aluminium causing greater plastic deformation than would be present in the peel test. Supplementary tests on this aluminium with the load cell and roller bar offset by 25 mm (see Figure 7) gave plastic work values similar to those obtained from the soft (B.S.3L61) aluminium shown in Figure 8. This then indicates that

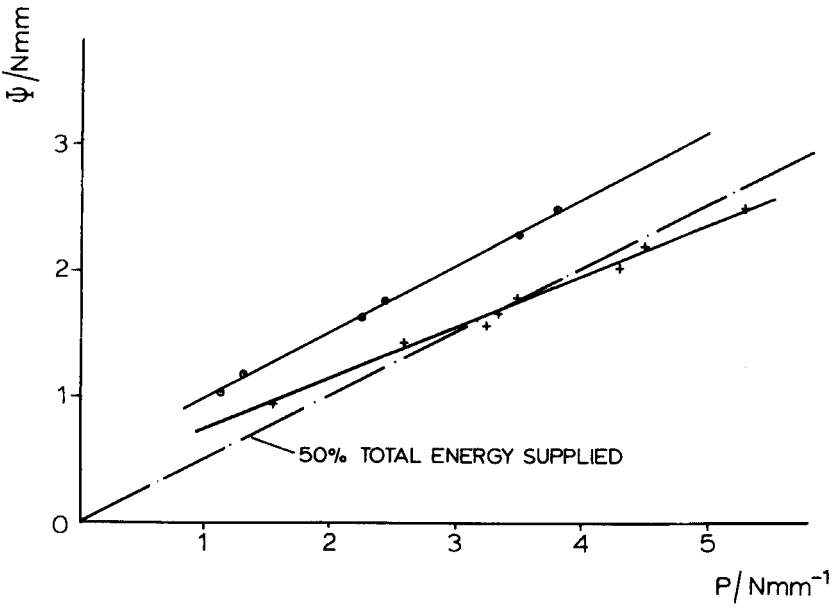

FIGURE 8 Variation of work in plastic deformation (Ψ) with applied load (P) for different aluminiums (⊙2024-T3; + BS 3L61).

the energy dissipated in plastic deformation of the flexible adherend is similar in peel tests A and B, even though the yield stress of one is an order of magnitude higher, and thus undergoes less plastic deformation than the other. This is because the plastic work is a function of both the stress level and plastic deformation in the material and, although the 2024-T3 experiences only small plastic deformation, it yields at high levels of stress. The converse is true of the B.S.3L61 aluminium. Moreover, this energy dissipated in plastic deformation is a considerable proportion, about 50%, of the total energy supplied during peeling.

Appendix I outlines an approximate method of calculating these plastic work values and has been adapted from Ref. 18. From the results, it can be seen that the measured values are of the expected order of magnitude, and reasonable correlation exists between the theoretical and observed results, considering the assumptions made in the theoretical calculations.

The effect of this plastic deformation by the flexible adherend in the 90° peel test is to increase the apparent work to fracture of the adhesive. For the configurations tested above, the apparent work to fracture is approximately doubled by the plastic deformation.

PEEL TEST ANALYSIS

Approach

As in the previous elastic analysis of the peel test,[1] both cracked and non-cracked configurations have been analysed. Owing to the incremental nature of the equations governing plastic behaviour, it is necessary to approach a full load solution in a series of small load steps. This involves considerably more computing time and consequently prevents such a degree of mesh refinement. However, since yielding eliminates the high stress gradients found in the elastic solution, it can be argued that such a degree of mesh refinement is no longer required.

Analyses were made of peel tests A and B, at peel angles of 90, 60 and 30 degrees up to peel loads of 5 N mm^{-1}, 8 N mm^{-1} and 25 N mm^{-1} respectively. These values were chosen to allow comparison with the series of peel tests described earlier. The uniaxial stress-strain characteristics of the aluminium adherends and the adhesive were modelled by cubic splined curves. Details of these can be found in Figures 2–4 and were considered in an earlier section.

Yielding of the aluminium adherends was modelled using the von Mises yield function (only dependent on deviatoric stress levels) while the adhesive behaviour was modelled using a modified paraboloidal yield criterion which is dependent on both deviatoric and hydrostatic stress levels. The significance and formulation of these criteria were discussed earlier (Yield Surfaces). For the modified von Mises function, it is necessary to supply the ratio of the initial yield stresses in compression and tension. Ishai[19] and Coppendale[20] have both determined this ratio for an epoxy adhesive over a range of strain rates: the former found that values of this ratio between 1.2 and 1.3 while the latter concluded that they lay between 1.26 and 1.29. Sultan and McGarry[21] tested a rubber modified epoxy system and reported ratios between 1.30 and 1.32. Thus it seems reasonable to use a value of 1.3 in this work.

The meshes, in the region around the bond end, used in the analysis are shown in Figure 9, the smallest elements are 0.1 × 0.25 mm. An adhesive thickness of 0.2 mm and adherend thicknesses of 0.57 mm and 0.64 mm for peel tests B and A respectively were taken, these corresponding to values used in the controlled series of peel tests discussed earlier. Adherend free lengths of 50 mm were used as this allows full development of the plastic region of deformation in the free adherend adjacent to the bonded region. The rigid substrate was modelled by constraining the appropriate adhesive nodes and a crack was introduced by giving the adhesive and adherend separate nodes on the free surface. There are a number of opinions about the type of singularity that is found in an elasto-plastic analysis of a cracked structure[22–24] and, in this work, standard elements were used in the region around the crack tip.

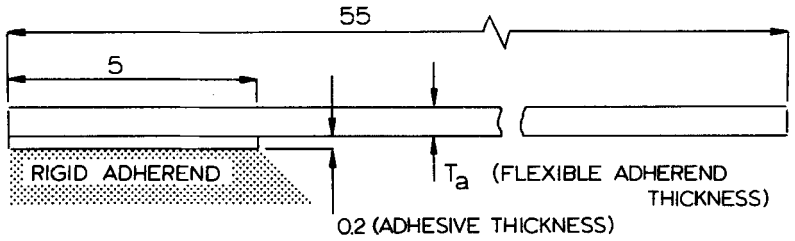

DETAIL OF MESH IN THE REGION AT THE BOND ENDS :

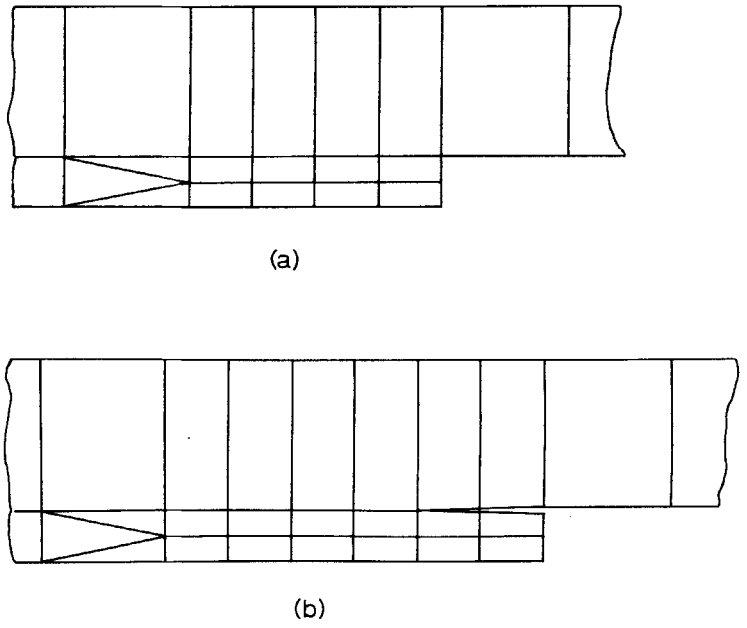

FIGURE 9 Details of meshes used in the elasto-plastic finite element analysis of the peel test ; ((a) non-cracked configuration ; (b) cracked configuration). All dimensions in mm.

For a plastic solution, it is necessary to apply the loads in a series of increments. The accuracy of the analysis depends on the number of increments used and this was checked by carrying out analyses of the same configuration with significantly more load increments. The similarity found between the two solutions indicated that the loading schemes used were satisfactory. It was

necessary to use a larger number of load increments for peel test B than for A. This was because of the greater plastic deformation encountered in peel test B.

Propagation of the Plastic Zone

The growth of the plastic zone in both the adhesive and the adherend was found to be similar for the various configurations of a particular peel test. Figures 10 and 11 show this growth for the cracked, 90°, A and B peel tests respectively. Contours drawn on the final deflected shapes of the configurations show the approximate positions of the plastic zone in the adherend and adhesive at various amounts of full load.

It can be seen in peel test B (Figure 11) that the adherend yields at very low values of applied load. Initial yield of the adherend occurs at about 1% of the full load at all the peel angles. Subsequent initial yield of the adhesive occurs at about 8% of the full load. However, in peel test A (Figure 10) adherend yielding occurs at higher load levels, initial yield being at about 16% of the full load. Adhesive yield precedes adherend yield, initial yield of the adhesive occurring at between 8% and 4% of the full load, yielding earlier at lower peel angles. The size of the adhesive plastic zone at full load is larger in peel test A than B.

Two points concerning the adherend yielding (in both peel tests) should be made. First, in the bonded region, material on the compressive side of the strip yields before the material on the other side. This is assumed to be due to the adhesive constraining the extension of the strip at the interface and so suppressing yield. The second point is the reversal of this process over the unbonded portion of the adherend. Here, the combination of bending and tension promotes yielding on the tensile side of the adherend.

Finally it should be stated that the size of the adhesive plastic zone increases at lower peel angles, although this is more apparent in peel test B than A. This appears to be in agreement with Coppendale[20] who reported extensive adhesive plasticity in an elasto-plastic analysis of the lap joint, which can be thought of as a low angle peel test.

Stress and Strain Distributions

Figure 12 shows the variation of the adhesive peel stress (σ_y) with distance from the crack tip, for the 90° cracked configuration of peel test A. The stresses were obtained from the Gauss points (points of numerical integration) closest to the adhesive-adherend interface. Similar distributions were found for the other configurations analysed. There are a number of points to note. First, plastic yielding causes a considerable reduction of the stress gradient near the crack tip. Similar distributions from the elastic analysis were shown to be singular in

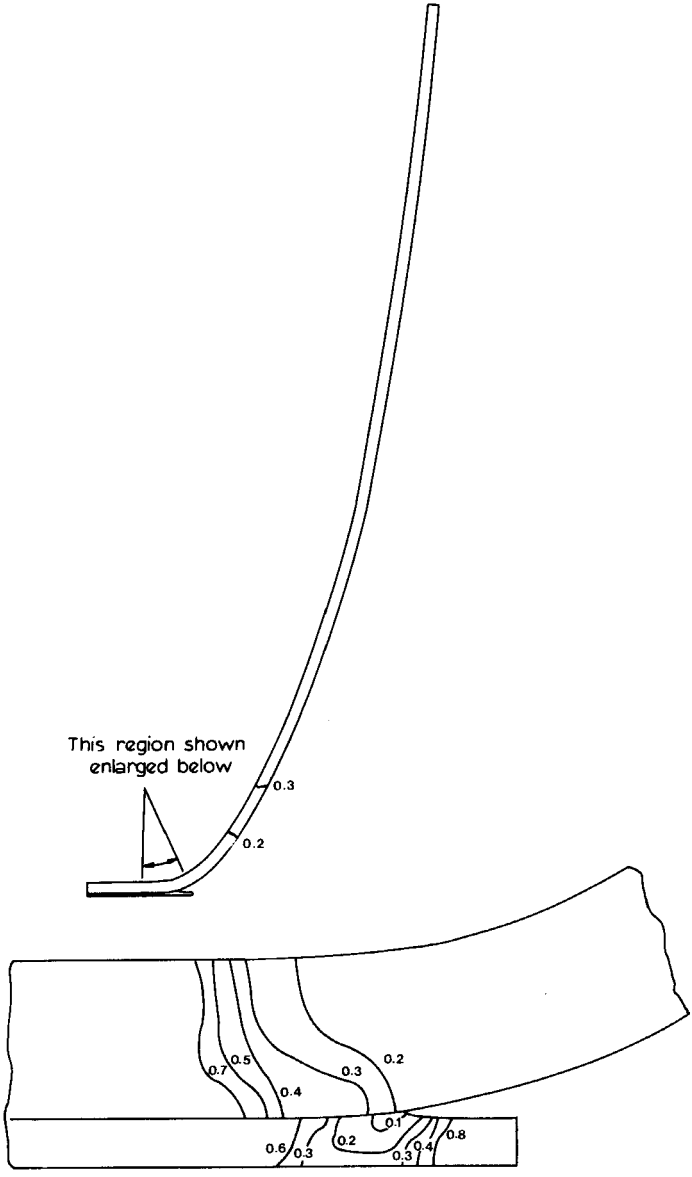

FIGURE 10 Growth of the plastic zone in peel test A.

this region.[10] Beyond the plastic zone, the shape of the stress distribution is as in the elastic analysis, a damped, harmonic function.

The stresses in Figure 12 exhibit a small degree of oscillation. It was found that this oscillation is more pronounced in the higher stressed regions, at high

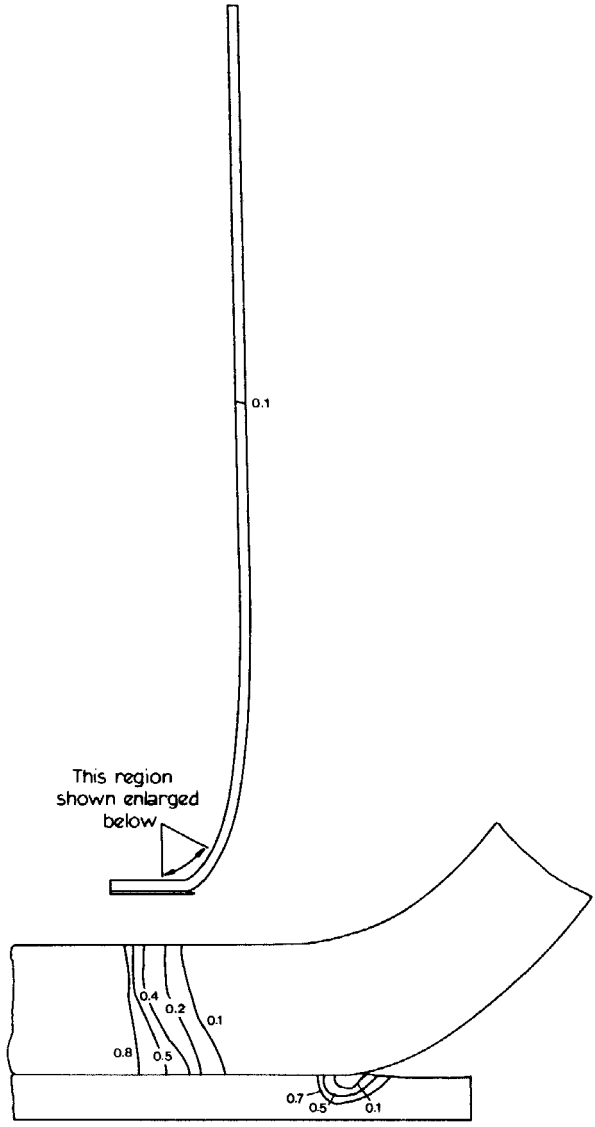

FIGURE 11 Growth of the plastic zone in peel test B.

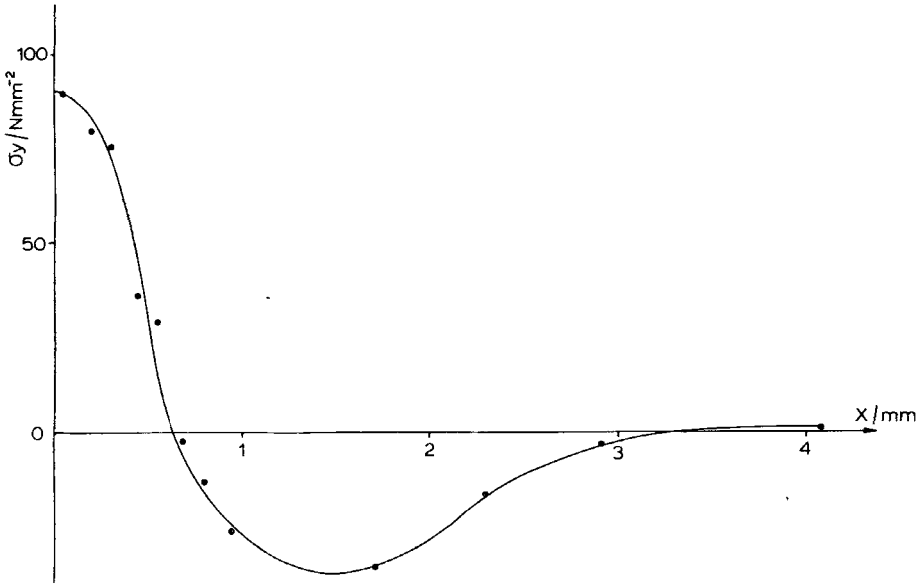

FIGURE 12 Variation of adhesive normal stress (σ_y) with distance (x) from the bond end.

peel angles and with the soft aluminium of peel test B. These oscillations appear to be independent of the solution procedure adopted as a number of variations were investigated and none produced a significant change in the stress distribution. Oscillations in the finite element analysis of bi-material systems have been noted by Anderson *et al.*[25] and, after some investigation, they decided that the oscillations were inherent in the mathematics of the finite element method.

The principal adhesive strain distribution, evaluated at the same positions as the stress distribution, from the analysis of the 90° cracked configuration of peel test A is shown in Figure 13. This is also typical of the other configurations analysed. For similar configurations, strains from peel test A are higher than those from peel test B. This is particularly so for the cracked systems and the use of a maximum adhesive strain as a failure criterion is considered in the next section. It is interesting to note that the oscillations associated with the stress distributions are no longer apparent. From Figure 13 it can be seen that, although the adhesive stress gradient is reduced near the crack tip, the strain distribution remains singular. Thus, to assume failure in the peel test at a critical value of adhesive strain is not particularly meaningful.

Vincent[26] suggested a failure criterion, based on an earlier idea by McClintock and Irwin[27] of failure when the strain at a certain distance from

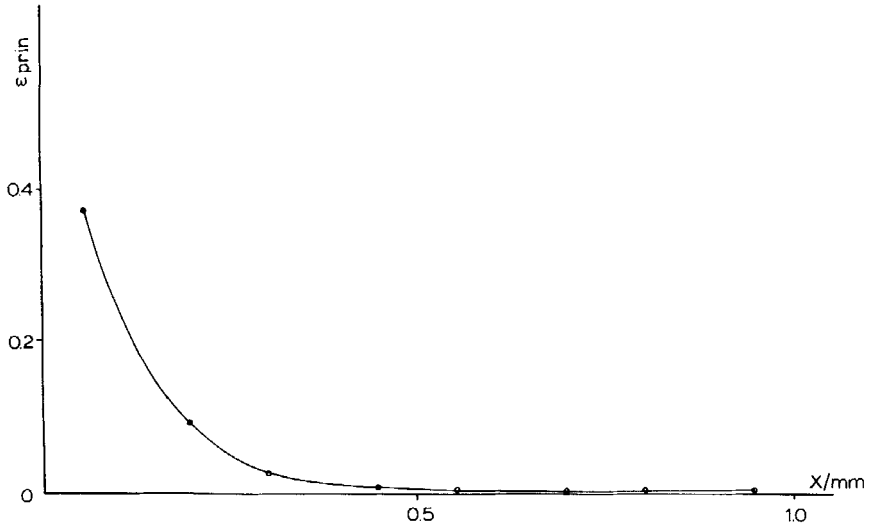

FIGURE 13 Variation of adhesive principal strain (ε_{prin}) with distance (x) from the bond end.

the crack tip reached a critical level. This idea is particularly appealing to the finite element analyst who can obtain values of strain at discrete points (of numerical integration) in the material surrounding the crack tip. Which particular values and distances to use in this analysis would necessitate a separate study and so, as a first attempt to use this type of criterion, adhesive strain values at the Gauss point closest to the crack tip have been used.

Effective Plastic Strain Failure Criteria

The effective plastic strain was introduced in an earlier section where it was used to determine the amount of work hardening and, by using the uniaxial stress-strain curve, the current level of the yield function. It is a product of both the stress and plastic strain levels and is used here as a failure criterion. Following the ideas outlined in the previous section, failure in the peel test has been assumed when the value of the adhesive effective plastic strain at the Gauss point closest to the crack tip reaches a critical level.

Figures 14 and 15 give details of how this strain varies, in peel tests A and B, as the load is increased. The load is represented as a fraction of the full load that is applied in each test (5 N mm^{-1}, 8 N mm^{-1} and 25 N mm^{-1} for peel angles of 90°, 60° and 30° respectively). By using the measured peel strength at a particular peel angle, it is possible to obtain the critical effective plastic strain and hence to predict failure at other peel angles.

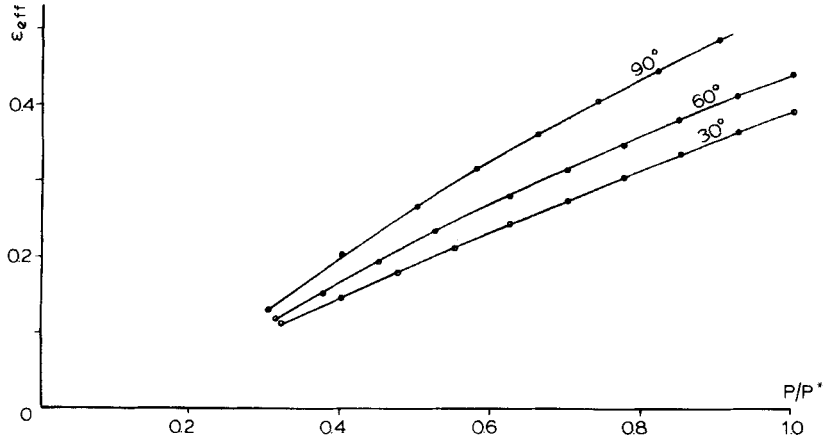

FIGURE 14 Variation with load (P) of the adhesive effective plastic strain (ε_{eff}) at the Gauss point closest to the crack tip for peel test A; (P^* = 5, 8 and 25 N mm^{-1} for peel angles of 90, 60 and 30 degrees respectively).

This can be illustrated for both the A and B peel tests. From the 30° peel angle strengths measured in the controlled peel tests predicted values of the 60° and 90° peel strengths can be found. These are summarised in Table I and comparison with the measured peel strengths indicates that the adhesive

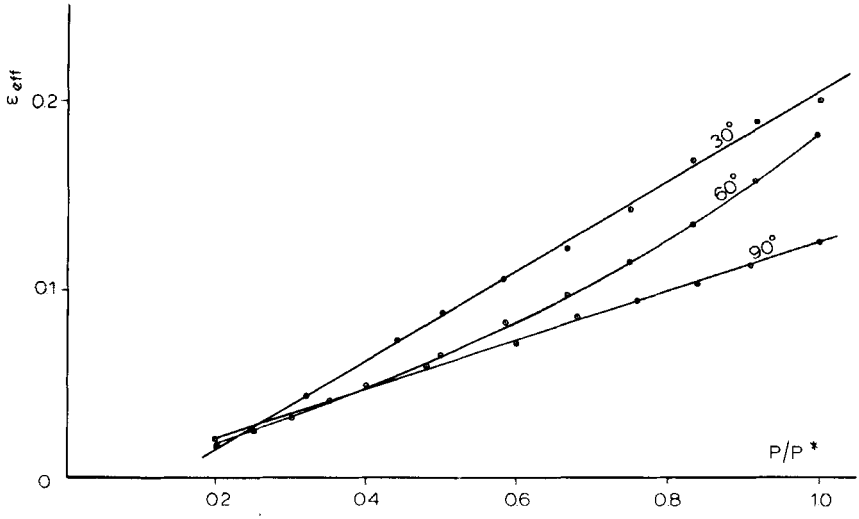

FIGURE 15 Variation with load (P) of the adhesive effective plastic strain (ε_{eff}) at the Gauss point closest to the crack tip for peel test B; (P^* = 5, 8 and 25 N mm^{-1} for peel angles of 90, 60 and 30 degrees respectively).

TABLE I

Predicted and measured peel strengths from the A and B peel tests

	Peel test A			Peel test B		
Peel angle	90°	60°	30°	90°	60°	30°
Predicted strength	3.3	6.5	23.2	7.1	8.6	22.5
Measured strength	4.3	7.3	23.2	6.0	9.4	22.5

effective plastic strains can be used successfully to predict the relative strengths of the same peel test.

However, values of adhesive effective plastic strain from peel test B are considerably lower than those from peel test A (compare Figures 14 and 15). This same feature was noted about the adhesive principal strain distribution in the last section. This implies a much larger difference between the peel strengths than was observed (Figure 6). There are a number of possible explanations for this.

a) It may not be correct to determine the adhesive effective plastic strain at the same point in the adhesive for both peel tests. It is possible that, because the adhesive plastic zones are larger in system A than B the adhesive effective plastic strain should be determined further from the crack tip in system A than B. This would lower the critical adhesive effective plastic strain found in peel test A and so reduce the differences in predicted strengths.

b) Analysis of the peel test with a very soft adherend is difficult (hence the stress oscillations noted) and may result in incorrect values of adhesive strain levels. This is supported by the fact that, at lower peel angles, the oscillations are not so severe and the differences in adhesive strains from the analyses of the A and B peel tests are not so significant.

c) A maximum adhesive strain to failure criterion may not be appropriate to the peel test, some other material parameter governing the peel test strength.

To investigate either of the first two options above would require subsequent analysis with a higher degree of mesh refinement around the crack tip. The last option is best assessed by completing a study investigating different material parameters and their effect on the peel test.

CONCLUSIONS

Various aspects concerning the elasto-plastic response of the peel test have been considered.

The amount of work expended in the plastic deformation of the adherend

has been experimentally assessed and shown to be a considerable proportion, about 50%, of the total energy supplied during peeling. Thus, the non-linear nature of the peel test, established by the elastic analysis, is significantly enhanced by plastic deformation for the two systems considered. A small increase in adhesive strength requiring a larger change in peel load (caused by the reducing moment arm) is further enhanced by the increase in plastic deformation of the adherend. Further, for these two systems, the work dissipated in plastic deformation was found to be similar suggesting that, for these systems, peel strengths based on energy considerations should also be similar.

Finite element analyses of the two peel tests have been made. Oscillations in the adhesive stress distributions have been noted. These only become significant when considering the soft aluminium of peel test B and have been found to reduce as the peel angle decreases. This suggests that the oscillations are related to the amount of "large displacement" involved. The oscillations were not present in the adhesive principal strain distribution and have been attributed to the mathematics of the finite element technique.

Adhesive plastic zone sizes are larger in peel test A than B and increase further at lower peel angles. The effective adhesive plastic strain has been used to predict the relative strengths of a peel test at various peel angles. However, it is not as satisfactory in predicting the relative strengths of the different peel tests; some suggestions have been made to account for this.

APPENDIX I

Theoretical approach to evaluating the work dissipated in plastic deformation of a bending strip

The plastic deformation outlined earlier has been modelled as a moving strip of material deforming around a stationary roller (Figure 16). This process involves plastic bending at point A and unbending at point B, a frictionless sliding over the region AB is assumed.

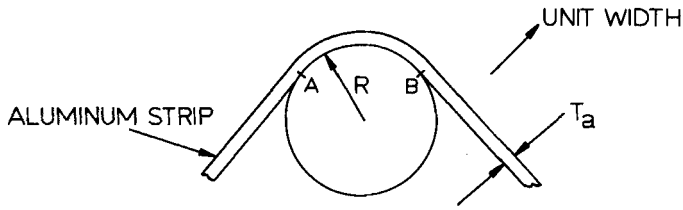

FIGURE 16 Outline of the configuration used in the calculation of the work expended in plastic deformation of a bending strip.

Assuming bending strains are much greater than the material yield strains and modelling the material as ideally plastic, the work expended in plastic bending and unbending for a unit movement of a unit width of strip is

$$\Psi = M_p\theta = M_p/(R + T_a/2)$$

where

$$M_p = T_a^2 Y/4$$

Y = yield stress

An estimate of the total plastic work required for plastic deformation of the systems discussed in the relevant section can be obtained by using the above formula and taking Y as a mean yield stress corresponding to the strain at a distance mid-way between the neutral axis and the outer fibres of the strip. In terms of the radius of curvature (R) of the bent portion the strain (ε) at this location is

$$\varepsilon = T_a/4R$$

The effect of superimposing tension changes the strains by less than 1% and hence has been neglected. Thus, by monitoring the radius of curvatures of the various tests outlined in the section on plastic deformation and referring to the stress-strain curves for the appropriate materials (Figures 2–4) values of plastic work, for strips of unit width, expended in bending and unbending a unit length of the strip can be found.

Specific results are summarised in Table II and these compare favourably with the observed values outlined in Figure 8.

TABLE II

Details from the theoretical calculations of the work dissipated in plastic deformation of a bending strip

Aluminium	Total load N	Bend radius (R) mm	Mean strain $= T_a/4R$	Mean yield stress N mm^{-2}	Plastic work N mm
†3L61	15.5	10.7	0.0133	58.0	8.58
3L61	33.4	5.7	0.0250	67.0	18.19
3L61	53.0	4.5	0.0317	71.0	24.10
‡2024-T3	12.1	45.0	0.0036	228.0	10.30
2024-T3	23.4	29.0	0.0055	295.0	20.61
2024-T3	36.8	24.0	0.0067	321.0	27.03

† $T_a = 0.57$ ‡ $T_a = 0.64$

References

1. A. D. Crocombe and R. D. Adams, *J. Adhesion* **12,** 187 (1981).
2. Ministry of Aviation, Aircraft Material Spec., *DTD 5577* (1965).
3. Amer. Soc. Test. Mat., *Floating roller peel resistance of adhesives, D3167-76* (1976).
4. J. J. Bikerman, *The Science of Adhesive Joints,* 2nd ed. (Academic Press, New York, 1968).
5. G. J. Spies, *Aircraft Engng.* **64** (1954).
6. A. J. Duke and R. P. Stanbridge, *J. Appl. Polym. Sci.* **12,** 1487 (1968).
7. A. J. Duke, *Int. Rubber Conf.,* Brighton, Paper C2-1 (1972).
8. A. N. Gent and G. R. Hamed, *Proc. Chem. Inst. Canada, Symp. Polymer Interfaces; Adhesion,* 1976, p. 165.
9. T. T. Wang and H. N. Vazirani, *J. Adhesion* **4,** 353 (1972).
10. A. D. Crocombe, *The non-linear stress and failure analysis of adhesive tests,* Thesis, University of Bristol (1981).
11. R. Raghava and R. Cadell, *J. Mat. Sci.* **8,** 225 (1973).
12. N. A. Peppiatt, *Some aspects of the paraboloidal yield surface,* Report AJ/4/13, University of Bristol (1976).
13. W. Johnson and P. B. Mellor, *Engineering plasticity* (van Nostrand Reinhold, New York, 1973).
14. O. C. Zienkiewicz, *The finite element method,* 3rd ed. (McGraw-Hill, New York, 1977).
15. O. C. Zienkiewicz, S. Vallippan and L. P. King, *Int. J. Num. Meths. Eng.* **1,** 75 (1969).
16. A. J. Kinloch and S. J. Shaw, *J. Adhesion* **12,** 59 (1981).
17. NAG Fortran Library Manual Mk 6, Section EO2, *Curve and surface fitting.*
18. W. Johnson and A. G. Mamalis, *Crashworthiness of vehicles, Part V* (Mech. Eng. Publs, 1978), p. 121.
19. O. Ishai, *J. Appl. Polym. Sci.* **11,** 963 (1967).
20. J. Coppendale, *The stress and failure analysis of structural adhesive joints,* Thesis, University of Bristol (1977).
21. I. N. Sultan and F. J. McGarry, *Polym. Eng. Sci.* **13,** 29 (1973).
22. A. S. Kobayashi, *Experimental techniques in fracture mechanics* **2** (Soc. Exp. Stress Anal., 1975).
23. N. Levy, P. V. Marcal, W. J. Ostergen and J. R. Rice, *Int. J. Fracture Mech.* **7,** 143 (1971).
24. J. W. Hutchinson, *J. Mech. Phys. Solids* **16,** 337 (1968).
25. G. P. Anderson, S. J. Bennett and K. L. de Vries, *Analysis and testing of adhesive bonds* (Academic Press, New York, 1977).
26. P. I. Vincent, *Polymer* **12,** 534 (1971).
27. F. A. McClintock and G. R. Irwin, *Plasticity aspects of fracture mechanics* (Amer. Soc. Test. Mat., STP 381, 1965), p. 96.